J. Fluid Mech. (2001), *vol.* 431, *pp.* 347–370. Printed in the United Kingdom

Chaotic advection in bounded Navier–Stokes flows

By IGOR MEZIĆ

Division of Engineering and Applied Sciences, Harvard University, Cambridge, MA 02138, USA

(Received 28 August 1998 and in revised form 20 August 2000)

We discuss mixing and transport in three-dimensional, steady, Navier–Stokes flows with the no-slip condition at the boundaries. The advective flux is related to the dynamics of the Navier–Stokes equations and a prediction is made of the scaling of the advective flux with the Reynolds number: the flux is expected to decay as the Reynolds number goes to infinity. This prediction is made via a Melnikov-type calculation together with boundary layer concepts through which the flow is split into an integrable and a small non-integrable part. The rate of decay is related to the details of viscous flow in boundary layers. The Melnikov function is related to the Bernoulli integral of the underlying Euler flow. The effects of molecular diffusivity are discussed and the effective axial diffusivity scaling predicted as a function of Reynolds and Péclet numbers. Using these ideas, we study the mass transport in the wavy vortex flow in the Taylor–Couette apparatus as a particular example. We propose an explanation of the observed non-monotonic behaviour of flux with increasing Reynolds number that was not captured in any of the previous models. It is shown that there is a Reynolds number at which the axial flux in the wavy vortex flow is maximized. At the low range of Reynolds numbers for which the wavy vortex flow is stable the flux increases, while for large Reynolds numbers it decreases. We compare these predictions with the available experimental and numerical data on the wavy vortex flow.

1. Introduction

In this paper we study an interesting phenomenon in chaotic advection that is a direct consequence of Navier–Stokes equations. We show that, in general, the size of chaotic regions in Navier–Stokes flows that are two-dimensional unsteady, three-dimensional steady or steady in a rotating frame decreases with the increase of the Reynolds number when the Reynolds number Re is increased and no instabilities are present. This is the consequence of the flow being split into an integrable Euler part and a possibly non-integrable viscous part. Applying the boundary layer singular perturbation concepts, the typical decay of the viscous contribution when $Re \to \infty$ is $Re^{-1/2}$ (Van Dyke 1964) and we show that the flux in such flows decays at this rate. As a particular example for which experimental data are available, we show that by increasing the Reynolds number in the wavy vortex flow, the flux between vortices (and thus the effective dispersion in the flow) admits an asymptotic expansion of the type $aRe^{-1/2} + bRe^{-1} + O(Re^{-3/2})$, where a, b are constant. Thus increasing the Reynolds number in this set-up decreases transport and mixing in the flow.

We discuss the experimental studies of this phenomenon done by Wereley & Lueptow (1998) and Desmet, Verelst & Baron (1996) and a numerical study by

Rudman (1997). Other experimental studies (Tam & Swinney 1987; Moore & Cooney 1995) concentrated more on the flux in the turbulent regime. The advective flux was examined by Wereley & Lueptow experimentally and Rudman numerically. In the study of Desmet *et al.* (1996) molecular diffusion effects were measured as well.

The first study of the change of chaotic advection properties with the Reynolds number was done by Bajer & Moffatt (1992) in the context of small Reynolds number flows between two concentric steadily rotating spheres. In that paper it was concluded that inertial effects (i.e. the increase of the Reynolds number) increased the chaotic advection in the flow for small Reynolds numbers. We investigate the other limit – that of large Reynolds numbers – and conclude that the opposite is true: the flow becomes more integrable with the increase in Reynolds number.

The theory that we provide is based on the perturbative Melnikov method. Holmes (1984) was the first to use the Melnikov method in the context of transport in three-dimensional fluid flows. This paper goes beyond Holmes' fundamental paper in several aspects: the Melnikov function is calculated in terms of the integral of motion of the unperturbed velocity field, thus making a connection to the recently developed theory of reduction by symmetry of volume-preserving flows (Mezić 1994; Mezić & Wiggins 1994; Haller & Mezić 1998). Yannacopoulos *et al.* (1998) observed that the symmetries of the flow can be divided in two types: *dynamical symmetries* which arise as a consequence of the equation of motion that the fluid satisfies and *geometrical symmetries* typically arising from the geometry of the container. We exploit these notions further here. We also use the theory of MacKay (1993) on minimum flux surfaces in three-dimensional, volume-preserving flows and the boundary layer theory that provides us with the size of the perturbation from an Euler flow.

The structure of the paper is as follows. In § 2, we review topics of integrability and chaos in three-dimensional incompressible Newtonian fluid flows. Flux through surfaces separating different regions of the flow is related to the dynamics of Navier–Stokes equations and an explicit prediction is made of the scaling of the advective flux with the Reynolds number at high Reynolds number for flows in which separating manifolds do not intersect boundary layers. The advective flux is expected to scale as $Re^{-1/2}$ as this is the correction to Euler flow inside the container due to viscous boundary layers. The Melnikov function is related to the Bernoulli integral of the underlying Euler flow. In the case when molecular diffusivity effects are important, we predict that the flux will scale as $c_1 Re^{-1/2} + c_2 Pe^{-1/2}$ for large Reynolds and Péclet numbers, where $Pe^{-1/2}$ is the thickness of the thermal boundary layer around the separating surfaces. In § 3, we predict that the advective flux in the wavy vortex flow in the Taylor–Couette apparatus at large Reynolds numbers admits an asymptotic expansion of the type $aRe^{-1/2} + bRe^{-1} + O(Re^{-3/2})$, where a, b are constant. The existence of a Reynolds number that maximizes flux in the apparatus is established. The effective diffusivity in the wavy vortex flow is predicted to scale as $D_{eff} \sim (C + Sc^{-1/2})/Re^{1/2}Sc^{1/2}$, where Sc is the Schmidt number. We compare the predictions with the experimental data in § 4 and conclude in § 5.

The experimental work that we discuss is not conclusive in terms of the power-law exponents for the flux: these studies were not done in order to test a particular power law and contain a small number of data points. Further experimental test of the predictions given will be necessary.

2. Boundary layers and non-integrability

In this section we discuss the connection between the structure of Navier–Stokes flows in the presence of solid boundaries at large Reynolds number and integrability

of particle motion in such flows. A connection is made between boundary layer theory and dynamical systems methods of computing flux.

2.1. *Integrability and chaos in 3-D incompressible steady flows*

In 1965 Arnold wrote a note on the integrability of three-dimensional Euler flows (Arnold 1966). In that note he asserted that three-dimensional Euler flows are integrable except in the case when vorticity and velocity are parallel. In fact, even when vorticity and velocity are parallel, but the constant of proportionality varies with space, such Beltrami flows are still integrable. Both of these facts were known to Lamb (Lamb 1932) and the surfaces spanned by non-parallel velocity and vorticity are known as Lamb surfaces (see Sposito 1997 for a detailed discussion of these). Based on the result on integrability, Arnold suggested the special solution of Euler's equation, the so-called ABC (Arnold–Beltrami–Childress) flows as possible non-integrable flows. These are spatially periodic Euler flows for which velocity is proportional to vorticity (i.e. they are Beltrami flows). Hénon 1966 perfomed a numerical simulation of ABC flows and found evidence of chaotic behaviour. Thus, the first results in the field of chaotic advection were based on the analysis of velocity fields that were smooth solutions of Euler equations. The flows discussed in chaotic advection studies in the 1980s and 1990s were kinematic models (e.g. the ABC maps of Feingold, Kadanoff & Piro 1988), solutions of Stokes equations (e.g. Bajer & Moffatt 1990; Stone, Nadim & Strogatz 1991), or weak solutions based on singular vortex distributions (e.g. Aref 1984; Rom-Kedar 1988; Rom-Kedar, Leonard & Wiggins 1990). Recently, a few studies (Ashwin & King 1995*a*, *b*; Yannacopoulos *et al.* 1998; Balasuriya, Jones & Sandstede 1997) appeared that took account of the restrictions imposed by the fact that Newtonian fluid flows satisfy Navier–Stokes equations.

One way of interpreting Arnold's suggestion on the importance of ABC flows is that viscous perturbations to Euler flows can be taken to be small away from the boundaries and, due to integrability of Euler flows that do not have velocity and vorticity proportional, chaotic motion can be only caused by an ABC-type flow. But, ABC flows are quite special. The condition that velocity is proportional to vorticity is very hard to establish experimentally (T. H. Solomon 1998, personal communication). In fact it can be shown rigorously that – in the region of the flow where inertial forces are dominant – the assumption that the steady flow can be split into dominant inertial part that solves the Euler equation and small viscous part leads to the conclusion that the Euler (inertial) part cannot be a chaotic ABC flow (Mezić 2000). In what follows, we paint quite a different picture of the physical nature of chaotic fluid particle motion in three-dimensional steady fluid flows: the cause of chaotic motion lies in viscous forces and, as Reynolds number increases to infinity, the extent of chaotic motion starts to decrease in a well-defined way.

2.1.1. *Geometrical and dynamical symmetries*

A sufficient condition for integrability (i.e. absence of chaotic motion) of a three-dimensional, incompressible vector field $\boldsymbol{v}$ is that it admits a volume-preserving symmetry (Mezić 1994; Mezić & Wiggins 1994; Haller & Mezić 1998), i.e. that there exists another incompressible vector field $\boldsymbol{s}$ such that the Lie bracket $[\boldsymbol{v}, \boldsymbol{s}]$ is zero. In Cartesian coordinates these conditions become

$$\left.\begin{aligned} [\boldsymbol{v}, \boldsymbol{s}] &= \boldsymbol{v} \cdot \nabla \boldsymbol{s} - \boldsymbol{s} \cdot \nabla \boldsymbol{v} = 0, \\ \nabla \cdot \boldsymbol{s} &= 0. \end{aligned}\right\} \tag{2.1}$$

When general incompressible $\boldsymbol{v}, \boldsymbol{s}$ satisfy (2.1) a function B defined by the equation

$$\nabla B = -\boldsymbol{v} \times \boldsymbol{s} \tag{2.2}$$

is an integral of motion for both $\boldsymbol{v}$ and $\boldsymbol{s}$, i.e. B is conserved on trajectories of both of these vector fields:

$$\frac{\mathrm{d}B}{\mathrm{d}t} = \boldsymbol{v} \cdot \nabla B = -\boldsymbol{v} \cdot \boldsymbol{v} \times \boldsymbol{s} = \boldsymbol{0} = -\boldsymbol{s} \cdot \boldsymbol{v} \times \boldsymbol{s} = \boldsymbol{s} \cdot \nabla B = \frac{\mathrm{d}B}{\mathrm{d}s},$$

where s is a time-like variable used to parametrize trajectories of the vector field $\boldsymbol{s}$. As an example of these general results, consider an incompressible vector field $\boldsymbol{v}$ which is symmetric with respect to translation along the z-axis, i.e. the velocity components (v_x, v_y, v_z) are independent of z. Let $\boldsymbol{s} = (0, 0, 1)$. Then (2.1) are clearly satisfied, as in components we have

$$\frac{\partial v_x}{\partial z} = \frac{\partial v_y}{\partial z} = \frac{\partial v_z}{\partial z} = 0, \quad \frac{\partial v_x}{\partial x} + \frac{\partial v_y}{\partial y} = 0,$$

and (2.2) becomes

$$\frac{\partial B}{\partial x} = v_y, \quad \frac{\partial B}{\partial y} = -v_x.$$

These equations clearly have a solution for B because $\boldsymbol{v}$ is incompressible. The cases of rotational and helical symmetry are treated similarly. The types of symmetries that result from symmetries of the flow domain have been called geometrical symmetries in Yannacopoulos *et al.* (1998).

Another type of symmetry that can arise is induced by the evolution equations of the fluid. Such a symmetry is for example the content of the Taylor–Proudman theorem for fast rotating flows (Batchelor 1967): when the Rossby number of a flow rotating around an axis with angular velocity Ω goes to zero, the velocity field satisfies

$$\Omega \cdot \nabla \boldsymbol{v} = 0.$$

Thus, such a flow possesses an integral of motion as (2.1) is satisfied with $\boldsymbol{s} = \Omega$. More generally, it is clear at once that (2.1) are satisfied by velocity $\boldsymbol{v}$ and vorticity $\boldsymbol{\omega} = \boldsymbol{s}$ of an Euler flow. Thus every Euler flow is integrable with the Bernoulli integral $B = (1/2)\boldsymbol{v}^2 + p/\rho$. The surfaces of constant B are called Lamb surfaces (see Sposito 1997). The topology of these surfaces inside a bounded analytical surface was shown to be toroidal or cylindrical by Arnold (1966), with the exception of separating surfaces between tori and cylinders.

Consider now an unbounded steady incompressible Navier–Stokes flow in $\mathbb{R}^3$. It satisfies

$$\boldsymbol{v} \cdot \nabla \boldsymbol{\omega} - \boldsymbol{\omega} \cdot \nabla \boldsymbol{v} = Re^{-1} \Delta \boldsymbol{\omega} \tag{2.3}$$

where Re is the Reynolds number of the flow. For such flows a regular perturbation expansion at large Reynolds numbers would read

$$\boldsymbol{v} = \boldsymbol{v}_E + Re^{-1} \boldsymbol{v}_1 + O(Re^{-2}), \tag{2.4}$$

where $\boldsymbol{v}_E$ satisfies Euler's equation of motion. This flow is thus $O(Re^{-1})$ away from an Euler flow. That Euler flow is integrable (Mezić 2000). Thus, the flux through any separating surfaces in this flow will be $O(Re^{-1})$, as was pointed out in the introduction of Mezić (1994), if $\boldsymbol{v}_1$ does not possess any symmetries.

The case of two-dimensional unsteady perturbaton of steady flows, which was treated rigorously in Balasuriya *et al.* (1997), can also be considered within the theory

outlined above. Two-dimensional steady flows of incompressible fluid are known to be integrable (i.e. the possibility of chaotic advection is excluded) due to the existence of a streamfunction. Consider an unsteady, two-dimensional Euler flow $\boldsymbol{v}$ that is time-periodic with period $2\pi/\beta$. Its vorticity $\boldsymbol{\omega}$ satisfies the two-dimensional Euler equation

$$\frac{\partial \omega}{\partial t} + \boldsymbol{v} \cdot \nabla \omega = 0,$$

which implies that ω is a quantity conserved on particle paths and thus the flow is integrable. In terms of the discussion above, $\boldsymbol{v}$ possesses a dynamical symmetry. To show this, let the domain in $\mathbb{R}^2$ in which the flow takes place be denoted by $\mathscr{D}$. Then the three-dimensional steady flow $\boldsymbol{v}_E = (v_x, v_y, \beta)$ is defined on $\mathscr{D} \times S^1$. For example, when $\mathscr{D}$ is a region in $\mathbb{R}^2$ whose boundary is a circle, then $\mathscr{D} \times S^1$ has the shape of a doughnut. The symmetry vector field $\boldsymbol{s}$ such that $[\boldsymbol{v}_E, \boldsymbol{s}] = 0$ is given by $\boldsymbol{s} = (\partial\omega/\partial y, -\partial\omega/\partial x, 0)$ (Haller & Mezić 1998). At large Re, $\boldsymbol{v}_E$ serves as the first term in the expansion of a Navier–Stokes flow. If there are no solid boundaries, then this expansion is (2.4).

This situation changes for Navier–Stokes flows for which there are viscous boundary layers. We investigate this case in the next subsection. It is interesting to point out here that we have not been able to construct any dynamical symmetries for fluid flows governed by the Stokes equation.

2.2. *Inner and outer expansions*

We consider the problem of determining the flux of fluid particles in and out of different flow regions in three-dimensional, steady Navier–Stokes flows in closed containers.

To be more specific, consider figure 1 which shows a sketch of separated regions of the flow in a region $\boldsymbol{R}$ with boundary $\partial\boldsymbol{R}$. We assume that the three-dimensional flow field is topologically of vortex-breakdown type, as shown in figure 1. Consider the flow in $\boldsymbol{R}$ governed by the steady Euler equation

$$\boldsymbol{v}_E \cdot \nabla \boldsymbol{v}_E = -\nabla p_E. \tag{2.5}$$

where the density $\rho = 1$ and a driving potential force has been absorbed into the pressure. The boundary condition on $\partial\boldsymbol{R}$ is $\boldsymbol{v} \cdot \boldsymbol{n} = 0$. By the discussion above, the velocity field is integrable and there is no flux of fluid between the regions denoted by I and II. We assume that the flow has swirl and two typical trajectories outside the vortex 'bubble' are shown. The surface Σ is filled with trajectories that approach the stagnation point A when time goes to negative infinity and approach stagnation point B when time goes to positive infinity. These are the heteroclinic orbits (Wiggins 1990). For large Reynolds numbers, outside the boundary layer, the solution to (2.5) is the first approximation to the Navier–Stokes velocity field governed by

$$\boldsymbol{v} \cdot \nabla \boldsymbol{v} = -\nabla p + \frac{1}{Re} \Delta \boldsymbol{v}, \tag{2.6}$$

where the velocity and pressure have been made non-dimensional, Re is the Reynolds number and the boundary condition on $\partial\boldsymbol{R}$ is $\boldsymbol{v} = \boldsymbol{v}_s$, where $\boldsymbol{v}_s$ is the surface speed (this condition may be local if, for example, the surface is fitted with microactuators able to change the local speed of the flow). We assume that in the presence of boundaries the velocity field can be split (Van Dyke 1964)

$$\boldsymbol{v} = \boldsymbol{v}_E + \boldsymbol{v}_P + \epsilon \boldsymbol{w}$$

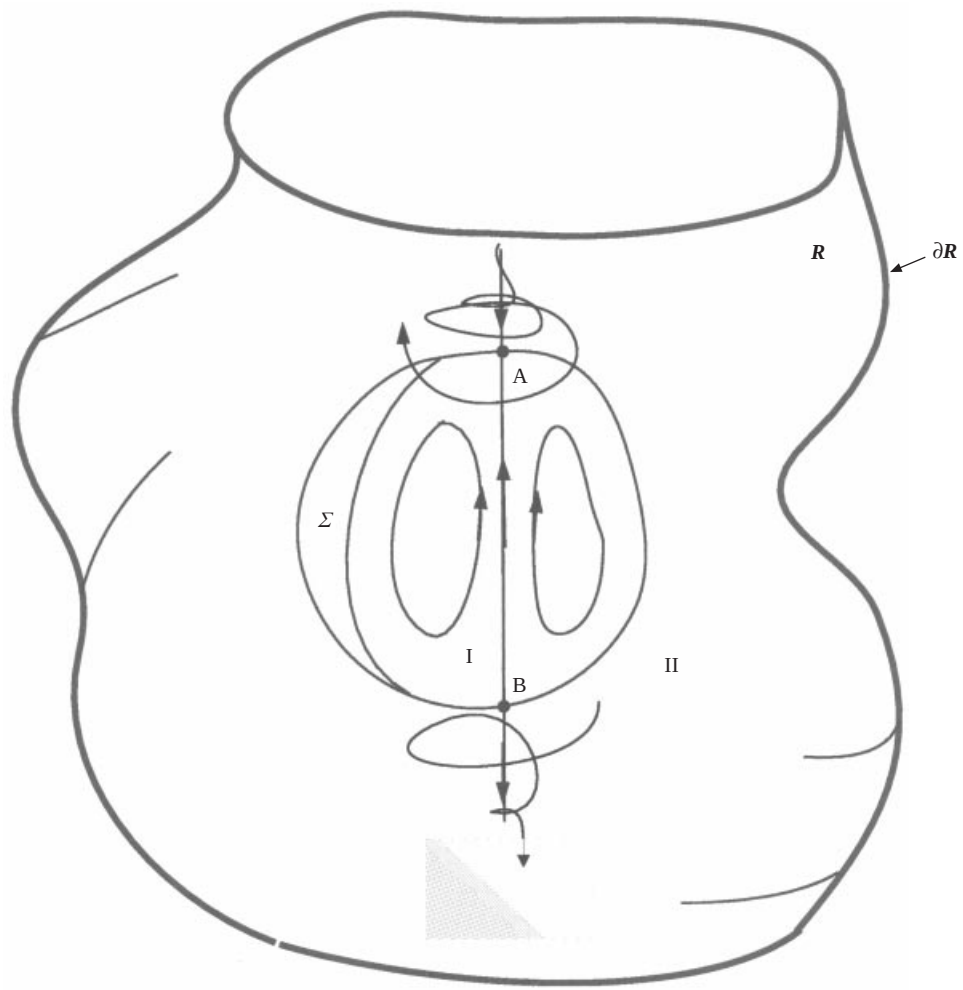

FIGURE 1. An Euler flow in a container with no symmetry.

where $\boldsymbol{v}_E$ satisfies Euler's equations of motion, $\boldsymbol{v}_P = \widetilde{\boldsymbol{v}_P} - \boldsymbol{v}_E$ inside boundary layers, where $\widetilde{\boldsymbol{v}_P}$ is the (Prandtl) solution that is valid inside the boundary layer of width $O(Re^{-1/2})$, and decays exponentially outside the boundary layers, and $\epsilon \boldsymbol{w}$ is the viscous correction such that $\epsilon = O(Re^{-1/2})$ for $Re \to \infty$. The inner expansion in the boundary layer is such that viscous effects are $O(1)$. Thus the velocity field in the boundary layer is, in the absence of geometrical symmetries, non-integrable. In the outer region the velocity field is

$$\boldsymbol{v} = \boldsymbol{v}_E + \epsilon \boldsymbol{w} + O\,(\exp)$$

where $O\,(\exp)$ denotes terms that are exponentially small in the distance to the boundary. This type of the velocity field splitting has recently been investigated rigorously for simple boundary geometries in two and three dimensions (Caflisch & Sammartino 1997, 1998). If the Euler velocity field $\boldsymbol{v}_E$ is not such that $c\boldsymbol{v}_E = \nabla \times \boldsymbol{v}_E$, where c is a constant (i.e. $\boldsymbol{v}_E$ is not Beltrami), then the Bernoulli integral $B = p + \boldsymbol{v}_E^2/2$ is non-trivial, i.e. is not constant in any three-dimensional subdomain. If we assume that surfaces separating I and II do not intersect boundary layers, then we can

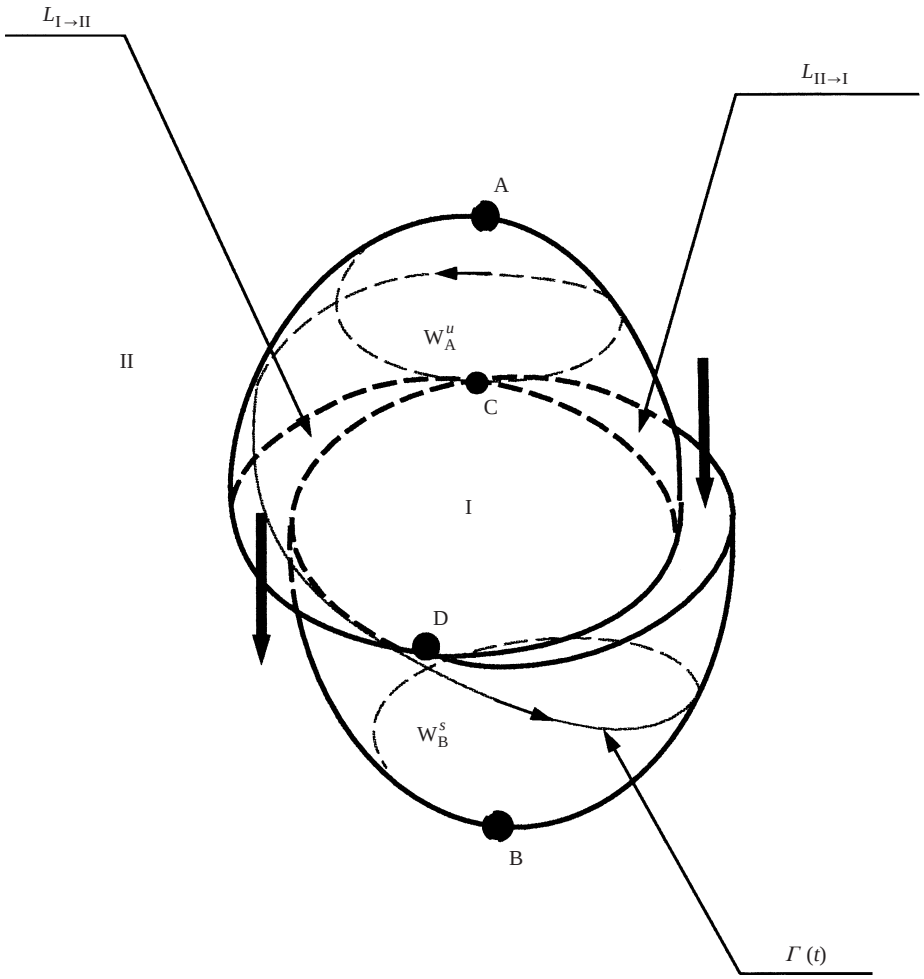

FIGURE 2. Surface of minimum flux for the perturbed Euler flow.

analyse the perturbed velocity $\boldsymbol{v} = \boldsymbol{v}_E + \epsilon \boldsymbol{w} + O(\exp)$ to determine whether there is any advective flux present.

The geometry of such a problem has been analysed in MacKay (1993) for steady perturbations and Holmes (1984) for unsteady perturbations. The fixed points A and B persist under perturbation, together with their unstable and stable manifolds W^u_{A} and W^s_{B} (Wiggins 1995) as sketched in figure 2. By the volume preservation, $W^u_{\mathrm{A}} \cup W^s_{\mathrm{B}}$ must intersect at least twice at the equator $z = 0$, and $L_{\mathrm{I}\to\mathrm{II}} \cup L_{\mathrm{II}\to\mathrm{I}}$ parts are added in order to form a closed bubble. MacKay (1993) proves that $S_p = W^u_{\mathrm{A}} \cup W^s_{\mathrm{B}} \cup L_{\mathrm{I}\to\mathrm{II}} \cup L_{\mathrm{II}\to\mathrm{I}}$ is a surface of locally minimum flux: in his development of the theory of transport for three-dimensional fluid flows he proves that a surface has locally minimum flux if it satisfies the following two conditions:

(i) It can be decomposed into surfaces P_i of unidirectional stationary algebraic flux $\mathscr{F}^i_{\mathrm{A}} = \int_{P_i} \boldsymbol{v} \cdot \boldsymbol{n} \mathrm{d}P_i$. The algebraic flux is stationary if and only if the boundary of the surface is invariant.

(ii) It has no 'sneaky returns', i.e. there are no orbits exiting and entering the surface with arbitrarily small paths travelled between exiting and entering.

On examining the sketch of intersections in figure 2 it is clear that the surface S_p

can be decomposed into two pieces that are spanned by two heteroclinic orbits and thus by Theorem 1 in MacKay (1993) both of these pieces have stationary algebraic flux. In addition, it does not have any 'sneaky returns' as the unperturbed vector field is $O(1)$ on the boundary of the bubble. By the volume preservation, $W^u_{\mathrm{A}} \cup W^s_{\mathrm{B}}$ must intersect at least twice, but having more intersections does not change the theory much. An expression for flux between different regions can be developed using Melnikov theory and we do this next. MacKay (1993) also relates flux to a Melnikov function, but in a way that is not useful for our purpose: owing to the particular form of the velocity field we consider, we write below the Melnikov function in terms of the Bernoulli integral of the underlying Euler flow.

For simplicity, let us assume that the separating surface is a sphere for the unperturbed Euler flow $\boldsymbol{v}_E$ which is symmetric with respect to rotation around vertical axis. Let us parametrize the unperturbed spherical bubble by the time t_0 along a heteroclinic orbit and its intersection with the equator of the unperturbed bubble, θ_0. Using the higher-dimensional Melnikov method similar to that developed by Gruendler (1985), Holmes (1984), the distance $d(\theta_0, t_0)$ between W^u_{A} and W^s_{B} is given by $d(\theta_0, t_0) = \epsilon M(\theta_0, t_0)/|\nabla B(\theta_0, t_0)| + O(\epsilon^2)$, where

$$M(\theta_0, t_0) = \int_{-\infty}^{\infty} \boldsymbol{w} \cdot \boldsymbol{\psi}^1 \times \boldsymbol{\psi}^2(\gamma_{\theta_0}(t - t_0))\,\mathrm{d}t,$$

$\boldsymbol{\psi}^2(\gamma_{\theta_0}(t - t_0)) = \boldsymbol{v}_E(\gamma_{\theta_0}(t - t_0))$, and $\boldsymbol{\psi}^1$ satisfies the variational equation along γ_{θ_0}

$$\dot{\boldsymbol{\psi}}^1 = D\boldsymbol{v}_E \cdot \boldsymbol{\psi}^1. \tag{2.7}$$

From the previous considerations, in an Euler flow the vorticity $\boldsymbol{\omega}$ satisfies (2.7) and we can put $\boldsymbol{\psi}^1 = \boldsymbol{\omega}$, thus obtaining

$$M(\theta_0, t_0) = -\int_{-\infty}^{\infty} \boldsymbol{w} \cdot \boldsymbol{v}_E \times \boldsymbol{\omega}(\gamma_{\theta_0}(t - t_0))\,\mathrm{d}t.$$

Note that $M(\theta_0, t_0)$ does not depend on ϵ. The integral converges because of the exponential convergence of $\boldsymbol{v}_E$ to 0 along the heteroclinic orbit (Wiggins 1990). For the Bernoulli integral B we have

$$\nabla B = -\boldsymbol{v}_E \times \boldsymbol{\omega}.$$

Thus,

$$M(\theta_0, t_0) = \int_{-\infty}^{\infty} \nabla B \cdot \boldsymbol{w}(\gamma_{\theta_0}(t - t_0))\,\mathrm{d}t.$$

In fact, as B is invariant along $\boldsymbol{v}_E$, and $\boldsymbol{v}_P$ decays fast outside of the boundaries

$$M(\theta_0, t_0) = \frac{1}{\epsilon}\int_{-\infty}^{\infty} \nabla B \cdot \boldsymbol{v}(\gamma_{\theta_0}(t - t_0))\,\mathrm{d}t,$$

and the Melnikov function is equal to the integral along the heteroclinic orbit of the flux through the Lamb surface of constant B that separates regions I and II.

The expression (2.2) for the Melnikov function can be derived directly by using geometrical methods of Guckenheimer & Holmes (1983) and Wiggins (1990). The distance between the stable and unstable manifolds can be expressed as

$$d(\theta_0, t_0) = \epsilon \frac{M(\theta_0, t_0)}{|\nabla B(\theta_0, t_0)|} + O(\epsilon^2).$$

The geometric flux through S is given by

$$\mathscr{F}_{CA} = \int_{L_{\mathrm{I}\to\mathrm{II}}\cup L_{\mathrm{II}\to\mathrm{I}}} |\boldsymbol{v}_{NS}\cdot\boldsymbol{n}|\mathrm{d}A$$

where $\boldsymbol{n}$ is the unit normal to the surface of the lobe $L_{\mathrm{I}\to\mathrm{II}}$ or $L_{\mathrm{II}\to\mathrm{I}}$ and $\mathrm{d}A$ its area element. Thus, to the first order in ϵ,

$$\mathscr{F}_{CA} = \epsilon \int_0^{2\pi} \frac{|M(\theta_0,0)|}{|\nabla B(\theta_0,0)|} v_z(\theta_0)\,\mathrm{d}\theta_0$$

where v_z is the velocity component in the direction of the vertical axis.

Recall that the surface S is the surface of locally minimum flux. Our calculation does not exclude the possibility that elsewhere, there is a surface that separates the apparatus into an inner and an outer part through which the flux is smaller than the flux through S, thus restricting the flux through the whole apparatus to be smaller. Strictly speaking, we have only proven that flux is smaller than ϵ. But intuitively, S is the surface through which flux is globally minimal and thus the flux scales as $\epsilon = Re^{-1/2}$ for large Reynolds numbers. This amounts to assuming that the bound we have obtained is optimal. The second term in the Navier–Stokes expansion scales as Re^{-1} and thus we expect that the flux has an asymptotic expansion

$$\mathscr{F} = aRe^{-1/2} + bRe^{-1}, \tag{2.8}$$

where a, b are constants.

The difference between making a heuristic argument for the perturbative order of the flux, like the one in § 2.1.1, and the Melnikov method is that the latter identifies surfaces that have locally minimum flux as the important ones to establish an upper bound for the flux and also gives an expression – $M(\theta_0, t_0)$ – that has to be non-zero in order for the bound to hold. If M is non-zero, no surface close to the surface of locally minimum flux has zero flux and, because of the structure of the unperturbed problem – the only surfaces splitting the cylinder in two domains being the separating surfaces – a conjecture can be made that the bound on the flux is sharp.

We will do a similar calculation in the context of the wavy vortex flow in the Taylor–Couette apparatus in § 3. In the case that we have considered above, the separating surfaces were outside the boundary layers. In the case of the wavy vortex flow the separating surfaces intersect the boundary layers and we have to make a separate argument that the splitting of Navier–Stokes flow at large Reynolds numbers as introduced above still holds.

The intersection of stable and unstable manifolds causes complicated motion in the surrounding region and, given specific expressions for the flow conditions for chaotic motion in Wiggins (1992*b*), could be checked to prove the existence of a zero measure set on which the dynamics of the system is chaotic.

2.3. *The molecular diffusion effects*

The above argument dealt with the purely advective effects. Assume that the fluid has molecular diffusivity D, with the Péclet number $Pe = Ul/D$, where U and l are the characteristic velocity and lengthscale of the flow. The molecular diffusion is then the second mechanism (besides chaotic advection) that affects the flux across the surface S_p. The flux induced by molecular diffusion is proportional to the width of the thermal boundary layer around the separating surface, $Pe^{-1/2}$. The fluxes induced by molecular diffusivity and chaotic advection can be added to yield the total flux

across S_p:

$$\mathscr{F} \sim aRe^{-1/2} + cPe^{-1/2},$$

where a, c are constants.

3. Bounded flows with shear layers emanating from the wall

In the previous section we discussed flux between different regions of steady flows whose separating manifolds do not intersect the boundary layer. There are many examples of flows in which this is not the case, such as laminar Taylor vortex flow between rotating concentric cylinders and wavy vortex flow that is steady in a rotating frame. Two complications arise when we want to extend our previous analysis to this case: first, it is not clear that the flow can still be separated into an Euler flow and a small viscous contribution; and secondly, flux across separating surfaces will have a contribution from the boundary layer flow that is not necessarily integrable. These issues are related to the the exact structure of the so-called shear layers emanating from the walls. This topic has been a subject of some debate, for example in the context of the flow induced by a cylindrical sphere rotating in a quiescent fluid (see e.g. Dennis, Ingham & Singh 1981, p. 377). In this section we first argue that the separation into Euler and viscous parts still holds by starting with an ansatz expansion into powers of $Re^{-1/2}$. We use this expansion to predict the structure of shear layers and then compare the results with available numerical data on the rotating sphere flow. Given that all the analytical predictions agree with numerical results of Dennis *et al.* (1981) we feel encouraged to apply the methods to wavy vortex flow, which has a similar structure, and study chaotic advection in that flow based on the expansions employed above.

Flux measurements in the wavy vortex flow contain a surprise: on increasing the Reynolds number, the flux first increases and then decreases (Wereley & Lueptow 1997). Previous models of this flow based on kinematic models and chaotic advection ideas (Broomhead & Ryrie 1988; Ryrie 1992; Rudolph, Shinbort & Lueptow 1998) are consistent in predicting monotonic increase. The study of Ashwin & King (1997) uses perturbation expansion near the onset of wavy vortices, and thus is based on Navier–Stokes dynamics, but does not give a prediction of flux vs. Reynolds number behaviour.

We show that the dynamics based decomposition of the velocity field predicts the non-monotonic behaviour observed in Wereley & Lueptow (1997) qualitatively correctly. We also compare the scaling based on restricted available data – our prediction being that at large Reynolds numbers advective flux in a three-dimensional wavy vortex flow between concentric cylinders has an asymptotic expansion of the form (2.8).

3.1. *Boundary layers and shear layers*

The purpose of this subsection is to establish some evidence that the splitting $\boldsymbol{v} = \boldsymbol{v}_E + \boldsymbol{v}_P + \epsilon \boldsymbol{w}$ still holds in the case when a separating surface intersects boundary layers. The geometry of the problem is shown in figure 3. Boundary layers are drawn next to the wall. The flow coming from two opposite directions at the boundary collides, leaves the boundary and goes into the shear layer. We will show that assuming expansion $\boldsymbol{v} = \boldsymbol{v}_E + \epsilon \boldsymbol{w} + O(\exp)$ for the flow outside boundary layers leads to predictions that are consistent with numerical experiments of Dennis *et al.* (1981) on boundary layer collision on a sphere rotating in a quiescent fluid. In the next

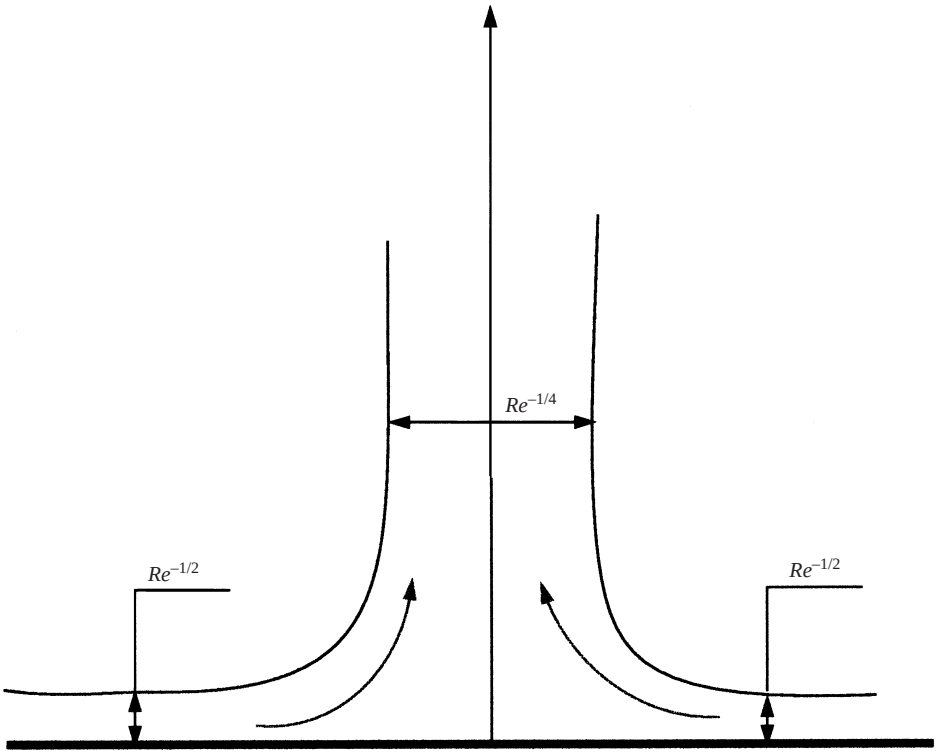

FIGURE 3. Structure of shear and boundary layers.

subsection we will apply these ideas to the wavy vortex flow in the Taylor–Couette apparatus.

Consider the steady flow within a shear layer. Assuming the expansion of the velocity field as above and neglecting terms that are exponentially small away from the boundary the Navier–Stokes equation (2.3) in the shear layer reads

$$(\boldsymbol{v}_E + \epsilon \boldsymbol{w}) \cdot \nabla(\boldsymbol{\omega}_E + \epsilon \boldsymbol{\omega}_w) - (\boldsymbol{\omega}_E + \epsilon \boldsymbol{\omega}_w) \cdot \nabla(\boldsymbol{v}_E + \epsilon \boldsymbol{w}) = \epsilon^2 \Delta(\boldsymbol{\omega}_E + \epsilon \boldsymbol{\omega}_w), \tag{3.1}$$

where $\boldsymbol{\omega}_E = \nabla \times \boldsymbol{v}_E$ and $\boldsymbol{\omega}_w = \nabla \times \boldsymbol{w}$. Under the assumption that the boundary layers are governed by shear and thus of order ϵ, the flow carries vorticity of order ϵ^{-1} into the shear layers. Thus, the equation at order ϵ^{-1} in (3.1) reads

$$\boldsymbol{v}_E \cdot \nabla \boldsymbol{\omega}_E - \boldsymbol{\omega}_E \cdot \nabla \boldsymbol{v}_E = 0, \tag{3.2}$$

which is, of course, just the steady Euler equation. At the next order we get

$$\epsilon(\boldsymbol{w} \cdot \nabla \boldsymbol{\omega}_E - \boldsymbol{\omega}_E \cdot \nabla \boldsymbol{w}) = \epsilon^2 \Delta \boldsymbol{\omega}_E. \tag{3.3}$$

We have already stated that vorticity in the shear layer comes from the wall boundary layer and thus it is expected that $\boldsymbol{\omega}_E = O(\epsilon^{-1})$. The left-hand side of (3.3) is thus $O(1)$. Let x be the coordinate along the wall and y the vertical coordinate increasing along the separation line. The right-hand side of (3.3) then becomes

$$\epsilon^2 \left(\frac{\partial^2 \boldsymbol{\omega}_E}{\partial x^2} + \frac{\partial^2 \boldsymbol{\omega}_E}{\partial y^2} \right).$$

It can be assumed that in the shear layer (and outside the boundary layer) $\partial^2 \boldsymbol{\omega}_E / \partial x^2 \gg$

$\partial^2 \boldsymbol{\omega}_E / \partial y^2$ and thus we have

$$\epsilon^2 \frac{\partial^2 \boldsymbol{\omega}_E}{\partial x^2} = O(1).$$

The thickness δ_x of the shear layer can be obtained from $\epsilon^2 \epsilon^{-1} / \delta_x^2 = 1$, i.e. $\delta_x = O(\epsilon^{1/2}) = O(Re^{-1/4})$. Thus, the shear layers are much thicker than the wall boundary layers, but the flow in them is inviscid to $O(Re^{-1/2})$.

Dennis *et al.* (1981) performed careful numerical experiments to determine the structure of boundary layers in the flow induced by a sphere rotating in an otherwise quiescent fluid at Reynolds numbers up to 5000. They state (Dennis *et al.* 1981, p. 376) that the thickness of the shear layer region is $Re^{-1/4}$ in contradiction to previous theories based on the existence of a recirculation zone in the collision region. From our analysis above, the change of vorticity in the horizontal direction, $\partial \boldsymbol{\omega}_E / \partial x = O(\epsilon^{-1} / \epsilon^{1/2}) = O(\epsilon^{-3/2}) = O(Re^{3/4})$. Dennis *et al.* (1981) observe the same scaling for the change of vorticity in the direction of θ that is equivalent to our x. Their numerical results support our contention that even for flows for which separating manifolds intersect boundary layers, the flow outside boundary layers can be written as $\boldsymbol{v} = \boldsymbol{v}_E + \epsilon \boldsymbol{w} + O(\exp)$. Thus, for large Reynolds numbers in steady flows with no geometrical symmetry the flux outside boundary layers again is written $\mathscr{F} = aRe^{-1/2} + bRe^{-1}$.

The boundary layer at the separation acquires thickness of size $Re^{-1/4}$ in the direction of y. It follows from the continuity equation that the component of $\boldsymbol{w}$ in the direction of x must be of the order $Re^{-1/4}$:

$$\frac{\partial \boldsymbol{w}_x}{\partial x} + \frac{\partial \boldsymbol{w}_y}{\partial y} = 0,$$

where $\boldsymbol{w}_y, y$ are $O(1)$ and x is $O(Re^{-1/4})$. Thus, the flux through the boundary layer is of the order $Re^{-1/2}$ or smaller and does not change the shape (although it could change the coefficients) of the expansion $\mathscr{F} = aRe^{-1/2} + bRe^{-1}$.

4. An example: the wavy vortex flow

Consider the flow of a Newtonian fluid between concentric cylinders where the inner cylinder is rotating and the outer is fixed. The wavy vortex flow (WVF) is the flow between concentric cylinders that occurs at just slightly higher Reynolds number Re_c than that for the Taylor vortices (Coles 1965; Marcus 1984; King *et al.* 1984; Wereley & Lueptow 1998). The flow is unsteady in the inertial frame of reference. At the onset of instability the WVF has the form of an azimuthal travelling wave perturbation to the Taylor vortex flow. The speed of the perturbation is somewhat less than half the rotational velocity of the inner cylinder, and in the frame of reference moving with the azimuthal wave the flow is steady. The WVF stays stable through an order of magnitude range of Reynolds numbers. For example, in Wereley & Lueptow's experiments with the gap between cylinder being 0.89 cm and the radius ratio 0.830 ± 0.003, Taylor vortices occur at $Re = 102$ and WVF is stable between Reynolds numbers of 131 and at least 1227. We will first discuss the advective transport of fluid at the high Reynolds number end.

4.1. *Decomposition of the velocity field*

We have discussed above that, even for flows with shear layers where vorticity generated at the boundaries enters the interior of the flow, the splitting into Euler

and small viscous parts should hold. Further evidence for this is the work of Marcus (1984) in which it is shown that, for sufficiently large Reynolds numbers, there are boundary layers at cylinder walls with the central part of the flow having essentially no gradient of momentum flux. Based on these considerations, we assume that outside boundary layers in the wavy vortex regime the flow can be decomposed as

$$\boldsymbol{v} = \boldsymbol{v}_E + \epsilon \boldsymbol{w} + O(\epsilon^2, \exp) \tag{4.1}$$

where $\boldsymbol{v}_E$ satisfies Euler equations of motion, and $\epsilon \boldsymbol{w}$ is the viscous correction such that $\epsilon = O(Re^{-1/2})$ for $Re \to \infty$. The Euler part $\boldsymbol{v}_E$ is then a steady flow that satisfies

$$[\boldsymbol{v}_E, \boldsymbol{\omega}_E + 2\Omega \boldsymbol{k}] = 0$$

where $\boldsymbol{\omega}_E = \nabla \times \boldsymbol{v}_E$, $\boldsymbol{k}$ is the unit vector in the axial direction and Ω the speed of the azimuthal wave. In addition we will assume that for the Euler part $\boldsymbol{v}_E \neq c\nabla \times \boldsymbol{v}_E$ for some constant c, i.e $\boldsymbol{v}_E$ cannot be Beltrami.

The scaling of the boundary layer that we have used is the same as that used by Batchelor (1960) in his Appendix of the paper by Donnelly & Simon (1960) in which they measured the torque for the Taylor vortex flow. Batchelor's prediction based on the viscous boundary layer scaling seemed to fit the torque data well. In Batchelor's case the structure of the shear layer is not important as he is interested in the torque only. For our argument, it was important to show that in shear layers the decomposition into an Euler part and a small viscous part still holds, as was done in the previous subsection.

An alternative scaling was offered by King *et al.* (1984) and Marcus (1984), based on marginal stability analysis. The flow in the boundary layer was assumed to be the Couette flow that was marginally stable to centrifugal instabilities. This analysis gave the scaling of the boundary layer to be $Re^{-2/3}$. Our assumption is then effectively that, at the higher range of Reynolds numbers, shear effects dominate over centrifugal effects in boundary layers.

4.2. *The Melnikov function*

The Euler part of the velocity field $\boldsymbol{v}_E$ is integrable due to the dynamical symmetry generated by the vorticity field $\boldsymbol{\omega} = \boldsymbol{\omega}_E + 2\Omega \boldsymbol{k}$. An integral of motion for $\boldsymbol{v}_E$ is given by $B = (1/2)(\boldsymbol{v}_E^2 + v_r^2) + p/\rho$ where $v_r = \Omega r_p$, $r_p = x^2 + y^2$ is the polar radius of a point and ρ is the density of the fluid, which is assumed to be a constant. Because of the cellular nature of the flow at finite Re, we assume that $\boldsymbol{v}_E$ has the structure indicated in figure 4. In fact, Wereley & Lueptow (1998) show that with increasing Reynolds numbers the flow acquires a simpler, more cellular structure – another argument for the decomposition into an integrable, cellular Euler flow and a small viscous part. In figure 4 we show the Euler flow decomposed into cells. The cell boundaries are two-dimensional manifolds Γ_U and Γ_D which are heteroclinic to one-dimensional manifolds γ_I^U, γ_O^U, and γ_I^D, γ_O^D on the inner and outer cylinder. For this flow, $\Gamma_U = W^u(\gamma_O^U) = W^s(\gamma_I^U)$ and $\Gamma_D = W^u(\gamma_I^D) = W^s(\gamma_O^D)$ where the stable manifolds of the one-dimensional curves are denoted by $W^u(\gamma_O^U), W^u(\gamma_I^D)$, and the unstable ones by $W^s(\gamma_O^D), W^s(\gamma_I^U)$. Γ_U and Γ_D are filled with heteroclinic orbits $\gamma_{\theta_0}^U(t), \gamma_{\theta_0}^D(t)$ that are labelled by the azimuthal coordinate θ_0 of their intersection with a plane $r_0 = const$. There is no flux between the cells in this integrable Euler flow. The flow $\boldsymbol{v}_E + \epsilon \boldsymbol{w}$ has the structure at the boundaries of the cells shown in figure 5. The stable and unstable manifolds of the one-dimensional manifolds on the boundary do not coincide any more. The distance between these two manifolds can be approximately calculated by the Melnikov method, as done above. The Melnikov

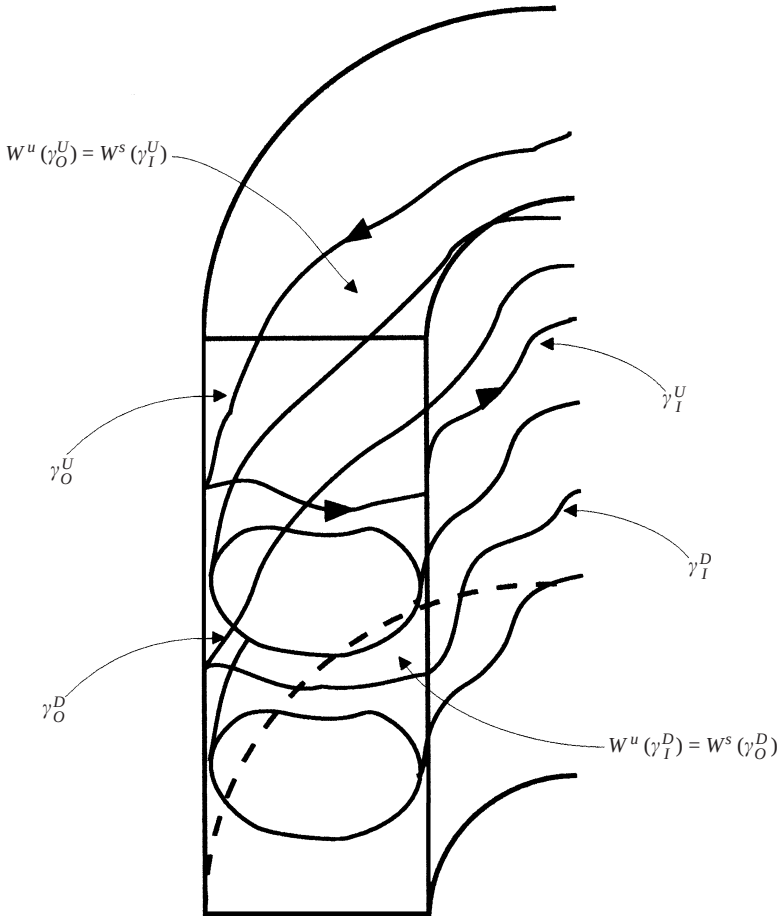

FIGURE 4. An Euler flow between concentric cylinders.

function can again be represented in terms of the Bernoulli integral of the Euler flow. The upper (lower) Melnikov function is given by

$$M^{U(D)}(\theta_0, t_0) = \int_{-\infty}^{\infty} \nabla B \cdot \boldsymbol{w}(\gamma_{\theta_0}^{U(D)}(t - t_0))\mathrm{d}t,$$

where t_0 runs along the heteroclinic orbit γ_{θ_0} and Melnikov theory is straighforwardly adapted for stable and unstable manifolds of periodic orbits. Note that $M^{U(D)}(\theta_0, t_0)$ does not depend on ϵ. The integral converges because of the exponential convergence of ∇B to 0 along the heteroclinic orbit (Balasuriya, Mezić & Jones 2000).

4.3. *The flux*

We are interested in the axial flux of fluid in the apparatus. If we consider any region in the apparatus bounded at the sides by cylinders and from above by surfaces (like the cells in the Taylor vortex flow), the total flux into the region through say the top surface must be equal to the flux from the cell to the region above the top surface, due to incompressibility. But, for dispersion processes, it is the one-sided ('geometric') flux that matters. In particular, if we find a surface that splits the space inside the apparatus in two parts and that surface can be shown to have locally minimum flux, we obtain an upper bound on the rate of transport (MacKay 1993).

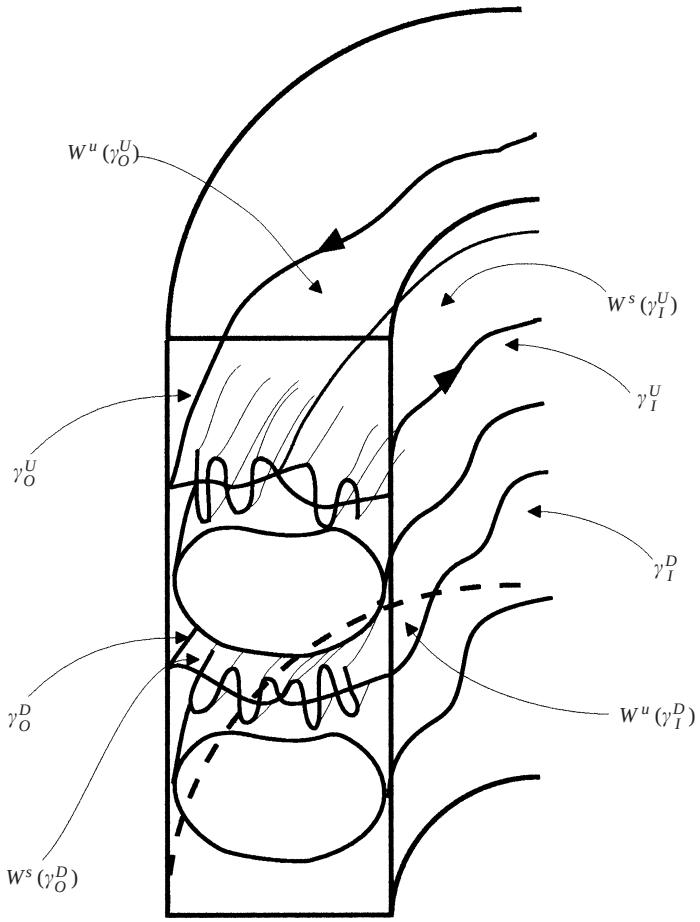

FIGURE 5. Wavy vortex flow in a rotating frame.

In figure 6 we show a locally minimum flux surface for $\boldsymbol{v}_E + \epsilon \boldsymbol{w}$. Its boundaries are the invariant lines γ_I and γ_O of the flow on the inner and outer cylinders. Consider now the intersection of the stable manifold $W^s(\gamma_I)$ of γ_I and the unstable manifold $W^u(\gamma_O)$ of γ_O. They intersect in trajectories defined by the zeros of the Melnikov function. Let us fix the $\theta_0 = 0$ plane and record its intersection with the stable manifold of γ_I and the unstable manifold of γ_O. We denote the point of intersection of these three surfaces as PIP. Then the surface that we seek is formed by the piece of the stable manifold that extends from γ_I to the trajectory h that passes through PIP and the piece of unstable manifold that extends from γ_O to h, together with the piece of the plane $\theta_0 = 0$ between the stable and unstable manifolds. This surface splits the solid annulus in two parts, denoted by I and II. Fluid in II can pass to I only through the lobe $L_{\mathrm{II}\to\mathrm{I}}$ that is bounded by pieces of stable and unstable manifolds in the plane $\theta_0 = 0$ that stretch from PIP to point C shown in figure 6. In the same way, fluid in I can pass to II only through the lobe $L_{\mathrm{I}\to\mathrm{II}}$. Checking again the requirements from MacKay (1993) it is not hard to see that S is a minimum flux surface. In particular, if PIP is chosen away from the unperturbed zero-swirl surface (which exists due to the fact that we are working in the frame co-rotating with the wave speed), S consists of two surfaces of unidirectional flux lying between the heteroclinic orbit that passes

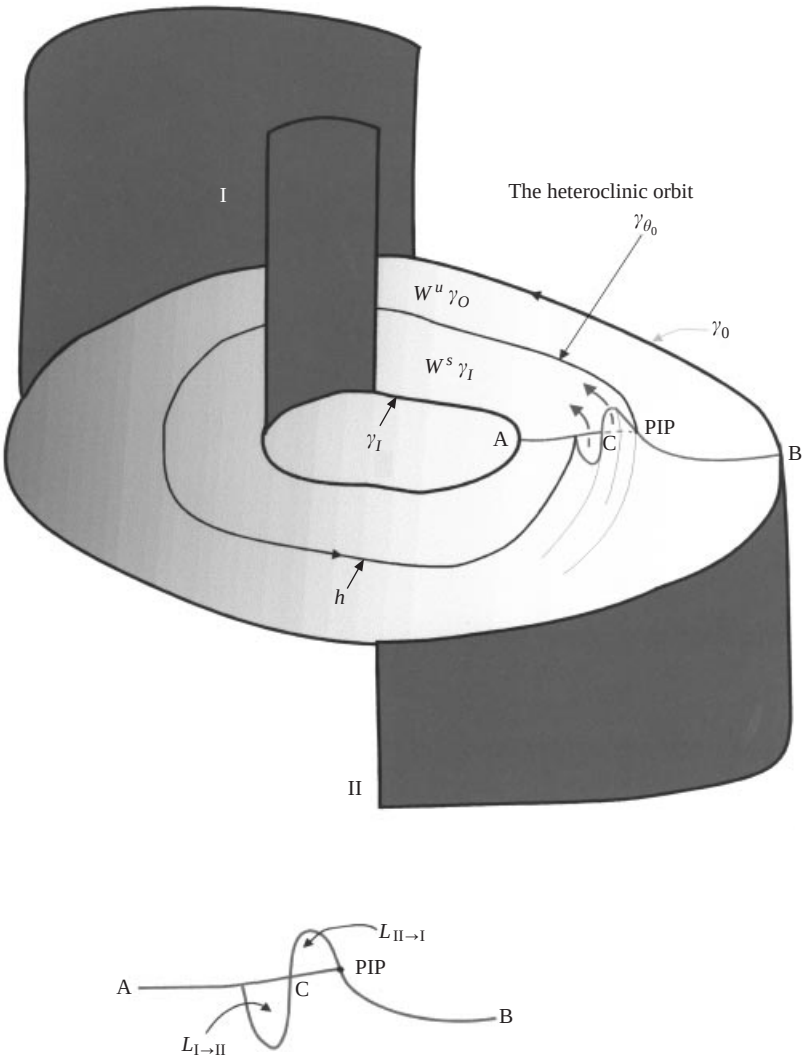

FIGURE 6. Minimum flux surface.

through PIP and periodic orbits at the boundary. It also has no 'sneaky returns'. The geometric flux through S is given by

$$\mathscr{F}_{CA} = 2\int_{L_{\mathrm{I}\to\mathrm{II}}} |\boldsymbol{v}_{NS}\cdot\boldsymbol{n}|\mathrm{d}A$$

where $\boldsymbol{n}$ is the unit normal to the surface of the lobe $L_{\mathrm{I}\to\mathrm{II}}$ and $\mathrm{d}A$ its area element. Thus, to the first order in ϵ,

$$\mathscr{F}_{CA} = 2\epsilon\int_{\mathrm{PIP}}^{\mathrm{C}} \frac{|M(\theta_0(l),t_0(l))|}{|\nabla B(\theta_0(l),t_0(l))|} v^{\theta}_{NS}(\theta_0(l),t_0(l))\mathrm{d}l$$

where $\mathrm{d}l$ is the piece of the stable manifold between PIP and C and v^{θ}_{NS} is the azimuthal velocity. C is a point at the boundary of the lobes as shown in figure 6. The flux is independent of the chosen t_0 as the choice of different t_0 only shifts the surface along the stable and unstable manifolds.

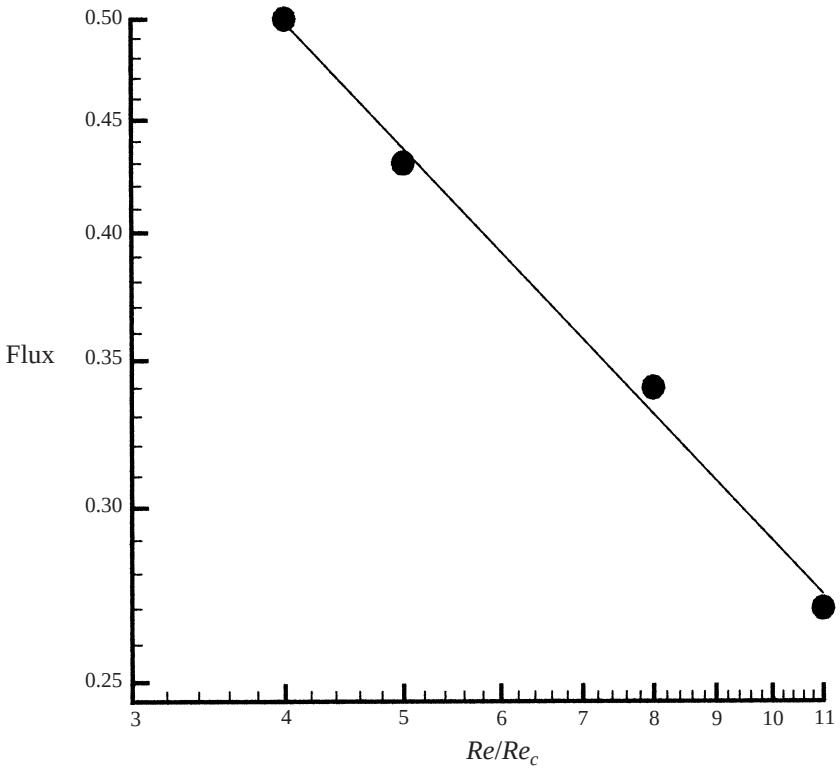

FIGURE 7. The least-squares fit to the Wereley–Lueptow data. The slope of the straight line is −0.59.

Thus, the flux scales as $\epsilon = Re^{-1/2}$ for large Reynolds numbers. The intersection of stable and unstable manifolds causes complicated motion in the surrounding region (Wiggins 1992*a*).

4.4. *Physical experiments*

Wereley & Lueptow's (1998) experiments are the only ones which measure the flux in the wavy vortex flow directly. All the other data that we consider are for effective axial diffusivity for which assumptions beyond those used in the theory above are needed. It is natural to try to model the motion outside the integrable Euler core of the vortices as a diffusive process. In fact Solomon, Tomas & Warner (1996) have shown that the estimates coming from this assumption are confirmed by experiments on two-dimensional, time-dependent chaotic flows. The axial effective diffusivity of this process scales in the same way as the flux $D_{eff} \sim aRe^{-1/2} + bRe^{-1}$.

In the measurements of Wereley & Lueptow (1998), the flux is obtained for the surface that has a minimum mean axial velocity at the given time, and thus represents a minimal flux surface. In the experiments, the flux between adjacent vortices first increases and then decreases. The data from the experiments in the decreasing flux regime are shown in figure 7. The least-square plot of the data gave a slope of −0.59, not far from the predicted value.

It is important to pick the right surface when measuring the flux. For example, taking a cross-cut through Taylor vortices would give positive geometric flux, but there

is really no effective axial flux as the boundaries of vortices are material boundaries. Choosing the boundary of the vortex as the flux surface would give the right result.

Desmet *et al.* (1996) measure the effective axial diffusivity for varying Reynolds number at various Schmidt numbers. They do not explicitly state the nature of the flow that they label 'laminar' as wavy vortex flow, but it is very likely that it is so (this was also discussed by Ohmura *et al.* 1997). When the Schmidt number is fixed, they find that the effective axial diffusivity scales as $Re^{-1/2}$.

4.5. *Numerical experiments*

Rudman (1997) has performed numerical experiments on advective dispersion in the WVF using a finite-difference method, for the parameter values corresponding to those of Coles' experiments (Coles 1965). In figure 8 we plot the data on effective axial diffusivity D_{eff} obtained by Rudman in the range of Reynolds numbers 486–756 where the axial effective diffusivity decays. The power law through the first couple of points of data is -0.6, while it seems much steeper for the last three points. Rudman observes that another frequency component is present in the numerical solution at $Re = 756$ and higher which actually prevented him from calculating dispersion at Reynolds numbers higher than 756. It might be that this causes the significant difference in the slope for the last three points. In addition, the relationship between the flux and D_{eff} could be less straightforward than simple proportionality: the flow in the boundary and shear layers, in particular the fact that it changes with the Reynolds number, could affect the scaling of the assumed diffusive process.

4.6. *Remark on the scaling of perturbation velocity*

As a final remark on the assumed scaling in the light of these experimental results we note that given the thickness of the boundary layer, our analysis below, strictly speaking, gives an *upper bound* on the flux. All the experimental results that we have discussed, except for the last three points on Rudman's plot, give an exponent that is smaller (i.e. bounded above) than $-1/2$, but bigger (i.e. bounded below) than $-2/3$. The exponent $-2/3$ was derived using marginal stability to centrifugal instabilities for Couette flow and would be an upper bound for the flux calculation. This suggests that the instability is shear-driven at high Reynolds numbers.

4.7. *Flux at the onset of the wavy vortex flow*

Our argument for the decay of the flux at the large Reynolds number end of the WVF existence is based on the dominance of inertial forces and the assumption that the boundary layers are shear-dominated in this range. Taylor vortex flow, the axisymmetric solution to which Couette flow is unstable, becomes itself unstable to a non-axisymmetric mode and WVF arises. At the Reynolds number at which this appears the viscous forces are still dominant and the main cause for the chaotic advection is breaking of the geometrical rotational symmetry around the z-axis.

The chaotic transport at the onset of the WVF has been studied by Broomhead & Ryrie (1988), Ashwin & King (1997) and Rudolph *et al.* (1998). Two of these studies utilize kinematic models. Broomhead & Ryrie's (1988) model is only qualitatively related to the WVF velocity field, while that of Rudolph *et al.* (1998) is based on PIV measurements of the velocity field. The work of Ashwin & King (1997) is a comprehensive study of particle motion based on perturbation expansions in Davey, DiPrima & Stuart (1968), but they do not discuss the dependence of flux on flow parameters.

According to Broomhead & Ryrie (1988) based on perturbation expansions in

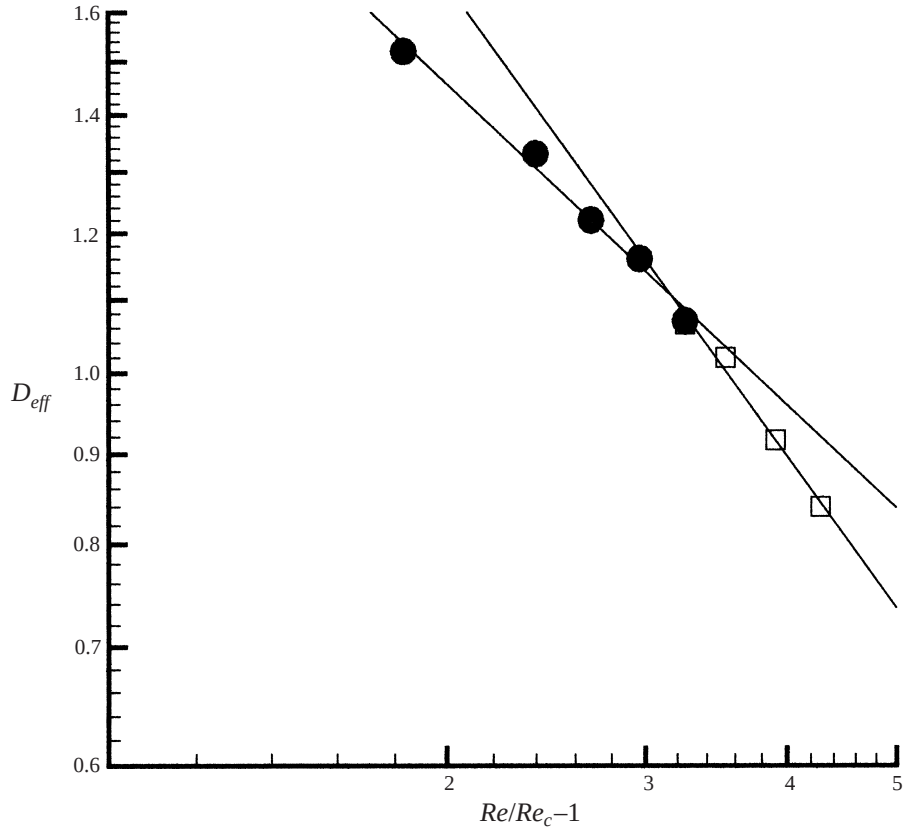

FIGURE 8. The least-squares fit to Rudman's data. The slope of the straight line through the black circles is −0.60, through the open squares −0.88.

Davey, DiPrima & Stuart (1968), the velocity field can be decomposed as

$$\boldsymbol{v}_{NS} = \boldsymbol{v}_{TVF} + \sqrt{Ta - Ta_c}\boldsymbol{u}$$

where Ta is the Taylor number in the apparatus. In this case $\boldsymbol{v}_{TVF}$ is the velocity field of the Taylor vortex flow and $\boldsymbol{u}$ is the wavy contribution. The velocity field $\boldsymbol{v}_{TVF}$ is integrable due to the rotational symmetry (this falls into the class of geometric symmetries discussed earlier). In this case, the Reynolds number at which WVF is stable is at its low end, so the effects of dynamical symmetry are much smaller than those of the rotational symmetry. An integral of motion B_R for $\boldsymbol{v}_{TVF}$ is given by (Haller & Mezić 1998)

$$\nabla B_R = \boldsymbol{v}_{TVF} \times \boldsymbol{g}, \tag{4.2}$$

where $\boldsymbol{g}$ is the infinitesimal generator of the rotational symmetry group, given by $\mathrm{d}r/\mathrm{d}s = 0, \mathrm{d}\theta/\mathrm{d}s = 1, \mathrm{d}z/\mathrm{d}s = 0$. The structure of $\boldsymbol{v}_{TVF}$ is very similar to that shown in figure 4, except that the separating manifolds are given by $z = const.$ planes. The upper (lower) Melnikov function is given by

$$M^{U(D)}(\theta_0, t_0) = \int_{-\infty}^{\infty} \nabla B_R \cdot \boldsymbol{u}(\gamma_{\theta_0}^{U(D)}(t - t_0))\mathrm{d}t.$$

The integral converges because of the exponential convergence of ∇B_R to 0 along the heteroclinic orbit (Balasuriya *et al.* 2000). This result is valid for all volume-preserving

flows when there is a volume-preserving symmetry for the unperturbed flow and we are interested in calculating flux across separating manifolds. Note that we do not need to compute B_R in order to calculate the Melnikov function. Using (4.2) we get

$$M^{U(D)}(\theta_0, t_0) = \int_{-\infty}^{\infty} \boldsymbol{v}_{TVF} \times \boldsymbol{g} \cdot \boldsymbol{u}(\gamma_{\theta_0}^{U(D)}(t - t_0))\mathrm{d}t.$$

Thus, for small perturbations the flux is proportional to $\sqrt{Ta - Ta_c}$, and initially increases. This conclusion was also reached in Broomhead & Ryrie (1988). Our treatment of the Melnikov calculation is simpler because we do not base it on the two-dimensional Poincaré map but on Gruendler's (1985) theory coupled with use of the underlying integrals of motion as described in § 2. Thus, the technical problems related to the fact that it is not possible to form a Poincaré map because of the existence of the co-rotating surface are not present. These problems were resolved in Broomhead & Ryrie (1988) using different methods.

While we have shown that the flux is expected to increase at the onset of WVF and is expected to decrease at the high end of the Reynolds number consistent with the stable WVF, it is not guaranteed that the flux has one maximum in this range. In fact Wereley & Lueptov's data show oscillations in the region betwen monotone increase and monotone decay. Rudman's numerical data, on the other hand, show only one extremum with the effective diffusivity first increasing with the appearance of WVF and then decreasing.

4.8. *The effect of molecular diffusion*

Assume that the fluid has molecular diffusivity D. The molecular diffusion is the second mechanism (besides chaotic advection) that affects the flux across the surface S. If there is no mean axial flow in the apparatus, and no 'accelerator modes' (Mezić, Brady & Wiggins 1996), the thermal boundary layer induced by molecular diffusion is proportional to $\sqrt{D}$ (Shraiman 1987) at large Péclet numbers. The fluxes induced by molecular diffusivity and chaotic advection can be added to yield the total flux. In non-dimensional terms the scaling of the axial effective Péclet number is thus given by

$$Pe_{eff}^{-1} \sim c_1 Re^{-1/2} + c_2 Pe^{-1/2} \tag{4.3}$$

where $Pe = ReSc$, $Sc = \nu/D$ and c_1, c_2 are constants. Thus,

$$Pe_{eff}^{-1} \sim \frac{C + Sc^{-1/2}}{Re^{1/2}Sc^{1/2}} \tag{4.4}$$

where C is a constant. In Desmet *et al.* (1996) the effective axial diffusivity was shown to fit the relationship

$$Pe_{eff}^{-1} \sim Re^{-1/2}Sc^{-1/2} \tag{4.5}$$

or

$$D_{eff} \sim Re^{-1/2}Sc^{-1/2}. \tag{4.6}$$

This type of relationship cannot hold for all the values of Re, Sc, as imagine an experiment in which $\nu = const.$ but D becomes smaller and smaller. Then, according to (4.6), the effective diffusivity D_{eff} would tend to zero. This cannot be, as there is a constant advective flux of the order $Re^{-1/2}$. Because of the similarity of (4.4) and (4.5) in some regimes, the data can seem to follow (4.5). This is easily seen by rewriting (4.3) as

$$Pe_{eff}^{-1} \sim c_1 Re^{-1/2} + c_2 Re^{-1/2}Sc^{-1/2}$$

where c_1 is on the order of the maximum of the Melnikov function (2.2). Thus, if $c_1 \ll c_2 Sc^{-1/2}$, $Pe_{eff}^{-1} \sim Re^{-1/2} Sc^{-1/2}$. The 'penetration model' discussed by Desmet *et al.* holds only approximately when the inter-vortex advective flux (the existence of which is verified in the experiments) is accounted for. It is important to notice that (4.3) has the right behaviour in both the limits $Re \to \infty$ and $Pe \to \infty$.

5. Conclusions

In this paper we have discussed the dependence of the advective flux on the Reynolds number in steady, three-dimensional Navier–Stokes flows with no-slip conditions at the boundaries. Using Melnikov theory, we have predicted that at large but finite Reynolds numbers the flux should scale as $Re^{-1/2}$, like the perturbation due to boundary layers to an Euler flow. Thus, the flux in steady flows should *decrease* as the Reynolds number is increased, at large Reynolds numbers. The particular example that we used for the illustration of the concepts is the wavy vortex flow in the Taylor–Couette apparatus which is steady in a rotating frame.

Advective flux is all-important in the case of transport and mixing of immiscible fluids (see e.g. Solomon *et al.* 1996). In the more common, miscible, situation we have to take into account molecular diffusivity. We have shown that in the general case for large Reynolds and Péclet numbers the flux will scale as $c_1 Re^{-1/2} + c_2 Pe^{-1/2}$. Our theory relies on a number of assumptions, the more important of which are: (i) the decomposition of Navier–Stokes vector fields into an Euler solution, a boundary layer solution and a small correction on the order of the size of the viscous boundary layer; (ii) the upper bounds on the flux obtained by constructing minimal flux surfaces (MacKay 1993) are assumed to be optimal.

We developed the theory in detail for the vortex-breakdown-type flow, for which separating surfaces do not intersect the boundary layer. We have also discussed wavy vortex flow (WVF) in the Taylor–Couette apparatus, for which separating manifolds are within shear layers that join the boundary layer. The Taylor vortex flow becomes unstable to a time-dependent wavy perturbation that is steady in the rotating frame. This new solution, called the WVF, loses stability at a Reynolds number an order of magnitude larger. After the onset of the wavy instability (i.e. for the low end of Reynolds numbers for which the WVF is stable) the inter-vortex flux increases (as observed already by Broomhead & Ryrie 1988) and we have shown that for the high end of the Reynolds numbers, for which the WVF is stable the flux decreases. Thus, our considerations also indicate the existence of an optimal Reynolds number that maximizes flux in the WVF. This prediction seems to be confirmed by the experimental results of Wereley & Lueptow (1998). We have also considered the case when molecular diffusivity is important and predicted its scaling. The experimental realization of the scalings that we get at the high Reynolds number end of the WVF existence depends on whether the scaling regime has been achieved. Depending on the other parameters of the problem, there is more hope that the scaling regime is reached if the WVF is stable for higher Reynolds numbers.

To calculate the flux we have employed the Melnikov method. We have related the Melnikov function to physical quantities such as the Bernoulli integral of motion for Euler flows. The Melnikov function can thus be interpreted as the integral over the unperturbed heteroclinic orbit of the flux of the Navier–Stokes flow through the 'unperturbed' Lamb surfaces which are the level sets of the Bernoulli integral. In the case of the volume-preserving (e.g. rotational) symmetry of the underlying flow, the Melnikov function was related to the cross-product of the unperturbed velocity field

with the infinitesimal generator of the symmetry group, thus making a connection to the recent geometrical theories of three-dimensional volume-preserving flows (Mezić 1994; Mezić & Wiggins 1994; Haller & Mezić 1998).

A theory similar to the one described here can be developed for time-dependent Navier–Stokes flows with a volume-preserving symmetry (e.g. rotational or translational) in a bounded container. A theory similar to the present one, for two-dimensional unbounded flows, was advanced by Balasuriya *et al.* (1997), with different scalings due to the absence of boundaries. There are a number of other fluid dynamical and magneto-hydrodynamical contexts in which similar ideas can be employed.

Let us close the paper with the observation that the experimental and numerical evidence for the phenomenon described here is far from being conclusive. The studies that have been done contain a restricted number of data points, and any scalings that are extracted suffer from the small sample defect. It is our hope that this paper will tempt more experimental work on the topic.

Thanks are due to Greg King, Pete Ashwin, George Rowlands and Thanasis Yannacopoulos for many useful discussions on Taylor vortex flows. Many thanks also to Murray Joe Rudman for providing more numerical data on the effective diffusivity. Fotis Sotiropoulos (re)directed my attention to vortex breakdown type flows by showing me his experimental and numerical results. This research was partially supported by the NSF grant DMS-9803555 and ONR grant N00014-98-1-0056.

REFERENCES

Aref, H. 1984 Stirring by chaotic advection. *J. Fluid Mech.* **143**, 1–21.

Arnold, V. I. 1966 Sur la géométrie differentielle des groupes de lie de dimension infinie et ses applications á l'hydrodynamique des fluides parfaits. *Ann. Inst. Fourier* **16**, 316–361.

Ashwin, P. & King, G. P. 1995*a* Azimuthally propagating ring vortices in a model for non-axisymmetric Taylor vortex flow. *Phys. Rev. Letts* **75**, 4610–4613.

Ashwin, P. & King, G. P. 1995*b* Streamline topology in eccentric Taylor vortex flow. *J. Fluid Mech.* **285**, 215–247.

Ashwin, P. & King, G. P. 1997 A study of particle paths in nonaxisymmetric Taylor–Couette flow. *J. Fluid Mech.* **338**, 341–362.

Bajer, K. & Moffatt, H. 1990 On a class of steady confined Stokes flows with chaotic streamlines. *J. Fluid Mech.* **212**, 337–363.

Bajer, K. & Moffatt, H. 1992 Chaos associated with fluid inertia. In *Topological Aspects of the Dynamics of Fluids and Plasmas* (ed. H. K. Moffatt, G. M. Zaslavsky, M. Tabor & P. Comte). Kluwer.

Balasuriya, S., Jones, C. K. R. T. & Sandstede, B. 1997 Viscous perturbations of vorticity-conserving flows and separatrix splitting. *Nonlinearity* **11**, 47–77.

Balasuriya, S., Mezić, I. & Jones, C. K. R. T. 2000 Weak Melnikov theory for 3-D Navier–Stokes flows. Preprint.

Batchelor, G. K. 1960 A theoretical model of the flow at speeds far above the critical. *J. Fluid Mech.* **7**, 416–418 (Appendix to Donnelly & Simon).

Batchelor, G. K. 1967 *An Introduction to Fluid Dynamics.* Cambridge University Press.

Broomhead, D. S. & Ryrie, S. C. 1988 Particle paths in wavy vortices. *Nonlinearity* **1**, 409–434.

Caflisch, R. & Sammartino, M. 1997 Navier–Stokes equations on an exterior circular domain: construction of the solution and the zero viscosity limit. *C. R. Acad. Sci. Paris* I **324**, 861–866.

Caflisch, R. & Sammartino, M. 1998 Zero viscosity limit for analytic solutions of the Navier–Stokes equations on a half-space: II. Construction of the Navier–Stokes solution. *Commun. Math. Phys* **192**, 463–491.

Coles, D. 1965 Transition in circular Couette flow. *J. Fluid Mech.* **164**.

Davey, A., DiPrima, R. & Stuart, J. 1968 On the instability of Taylor vortices. *J. Fluid Mech.* **31**, 17–52.

Dennis, S. C. R., Ingham, D. B. & Singh, S. N. 1981 The steady flow of a viscous fluid due to a rotating sphere. *Q. Mech. Appl. Math.* **34**, 361–381.

Desmet, G., Verelst, H. & Baron, G. V. 1996 Local and global dispersion effects in Couette–Taylor flow-II. Quantitative measurements and discussion of the reactor performance. *Chem. Engng Sci.* **51**, 907–931.

Donnelly, R. J. & Simon, N. J. 1960 An empirical torque relation for supercritical flow between rotating cyclinders. *J. Fluid Mech.* **7**, 401–416.

Feingold, M., Kadanoff, L. P. & Piro, O. 1988 Passive scalars, 3-dimensional volume-preserving maps and chaos. *J. Statist. Phys* **50**, 529–565.

Gruendler, J. 1985 The existence of homoclinic orbits and the method of Melnikov for systems in $\mathbb{R}^n$. *SIAM J. Math. Anal.* **16**, 907–931.

Guckenheimer, J. & Holmes, P. 1983 *Nonlinear Oscillations, Dynamical Systems and Bifurcations of Vector Fields*. Springer.

Haller, G. & Mezić, I. 1998 Reduction of three-dimensional, volume-preserving flows by symmetry. *Nonlinearity* **11**, 319–339.

Hénon, M. 1966 Sur la topologie des lignes de courant dans un cas particulier. *C. R. Acad. Sci. Paris* A **262**, 312–314.

Holmes, P. 1984 Some remarks on chaotic particle paths in time-periodic, three-dimensional swirling flows. *Cont. Maths.* **28**, 393–404.

King, G. P., Li, Y., Lee, W., Swinney, H. L. & Marcus, P. 1984 Wave speeds in wavy Taylor-vortex flow. *J. Fluid Mech.* **141**, 365–390.

Lamb, H. 1932 *Hydrodynamics*. Dover.

MacKay, R. S. 1993 Transport in 3-D volume-preserving flows. *J. Nonlinear Sci.* **4**, 329–354.

Marcus, P. S. 1984 Simulation of Taylor–Couette flow. Part 2. Numerical results for wavy-vortex flow with one travelling wave. *J. Fluid Mech.* **146**, 65–112.

Mezić, I. 1994 On geometrical and statistical properties of dynamical systems: Theory and applications. PhD thesis, California Institute of Technology.

Mezić, I. 2000 ABC flows as a paradigm for chaotic advection in 3-d, Preprint.

Mezić, I., Brady, J. & Wiggins, S. 1996 Maximal effective diffusivity for time periodic incompressible fluid flows. *SIAM J. Appl. Maths* **56**, 40–57.

Mezić, I. & Wiggins, S. 1994 On the integrability and perturbation of three dimensional fluid flows with symmetry. *J. Nonlinear Sci.* **4**, 157–194.

Moore, C. M. V. & Conney, C. L. 1995 Axial dispersion in Taylor–Couette flow. *AIChE J.* **41**, 723–727.

Ohmura, N., Kataoka, K., Shibata, Y. & Makino, T. 1997 Effective mass diffusion over cell boundaries in a Taylor–Couette problem. *Chem. Engng Sci.* **52**, 1757–1765.

Rom-Kedar, V. 1988 Part I: An analytical study of transport, mixing and chaos in an unsteady vortical flow. Part II: Transport in two-dimensional maps. PhD thesis, California Institute of Technology.

Rom-Kedar, V., Leonard, A. & Wiggins, S. 1990 An analytical study of transport, mixing and chaos in an unsteady vortical flow. *J. Fluid Mech.* **214**, 347–394.

Rudman, M. 1997 Mixing and particle dispersion in the wavy vortex regime of Taylor–Couette flow. *AIChE J.* **44**, 1015–1026.

Rudolph, M., Shinbrot, T. & Lueptow, R. M. 1998 A model of mixing and transport in wavy Taylor–Couette flow. *Physica* D **121**, 163–174.

Ryrie, S. C. 1992 Mixing by chaotic advection in a class of spatially periodic flows. *J. Fluid Mech.* **236**, 1–26.

Shraiman, B. I. 1987 Diffusive transport in a Rayleigh-Benard convection cell. *Phys. Rev.* A **36**, 261–267.

Solomon, T. H., Tomas, S. & Warner, J. L. 1996 Roles of lobes in chaotic mixing of miscible and immiscible impurities. *Phys. Rev. Lett.* **77**, 2682–2685.

Sposito, G. 1997 On steady flows with Lamb surfaces. *Intl. J. Engng Sci.* **35**, 197–209.

Stone, H. A., Nadim, A. & Strogatz, S. 1991 Chaotic streamlines inside drops immersed in steady Stokes flows. *J. Fluid Mech.* **232**, 629–646.

Tam, W. Y. & Swinney, H. L. 1987 Mass transport in turbulent Couette–Taylor flow. *Phys. Rev.* A**36**, 1374.

Van Dyke, M. 1964 *Perturbation methods in fluid mechanics.* Academic.

Wereley, S. T. & Lueptow, R. M. 1998 Spatio-temporal character of non-wavy and wavy Taylor–Couette flow. *J. Fluid Mech.* **364**, 59–80.

Wiggins, S. 1990 *Introduction to Applied Nonlinear Dynamical Systems and Chaos.* Springer.

Wiggins, S. 1992*a Chaotic Transport in Dynamical Systems.* Springer.

Wiggins, S. 1992*b Global Bifurcations and Chaos: Analytical Methods.* Springer.

Wiggins, S. 1995 *Normally Hyperbolic Invariant Manifolds in Dynamical Systems.* Springer.

Yannacopoulos, T., Mezić, I., King, G. & Rowlands, G. 1998 Eulerian diagnostics for Lagrangian chaos in three dimensional Navier–Stokes flows. *Phys. Rev.* E **57**, 482–490.